The role of subsurface oxygen in the selectivity enhancement of ethylene epoxidation on Ag–Cu Catalysts

ARTICLE · MARCH 2011

READS
25

3 AUTHORS:

Ngoclinh Nguyen
École Polytechnique Fédérale de Lausanne
21 PUBLICATIONS **84** CITATIONS
SEE PROFILE

Stefano de Gironcoli
Scuola Internazionale Superiore di Studi Ava…
192 PUBLICATIONS **12,073** CITATIONS
SEE PROFILE

Simone Piccinin
Italian National Research Council
42 PUBLICATIONS **434** CITATIONS
SEE PROFILE

THE JOURNAL OF PHYSICAL CHEMISTRY C

ARTICLE

pubs.acs.org/JPCC

Stability of Intermediate States for Ethylene Epoxidation on Ag−Cu Alloy Catalyst: A First-Principles Investigation

Ngoc Linh Nguyen,*[,†] Simone Piccinin,[†,‡] and Stefano de Gironcoli[†,‡]

[†]Scuola Internazionale Superiore di Studi Avanzati (SISSA), via Bonomea 265 I-34136, Trieste, Italy

[‡]CNR-IOM Democritos, via Bonomea 265 I-34136, Trieste, Italy

ABSTRACT: By means of first-principles density functional theory combined with atomistic thermodynamics, we have investigated the stability of several intermediates in the ethylene epoxidation reaction catalyzed by Ag−Cu alloys. We studied the surface phase diagrams of the low-index facets of Ag−Cu as a function of temperature and partial pressures of oxygen and ethylene, considering ethylene to be either physisorbed or chemisorbed in oxametallacycle and ethylenedioxy forms. We find that at high ethylene partial pressure or low temperature ethylene adsorbs as ethylenedioxy on a thin CuO layer formed on top of the silver particle. Subsurface oxygen can be present on the (111) facet at the interface between the CuO layer and silver. At temperatures and pressures relevant for industrial applications, though, the catalyst is not covered by ethylene and on all facets a thin CuO layers forms. The oxametallacycle intermediate is not predicted to be stable under any conditions. We have also investigated the shape of the catalyst particles as a function of the copper loading and temperature, showing that the dominant facet under conditions relevant for practical applications is the (100).

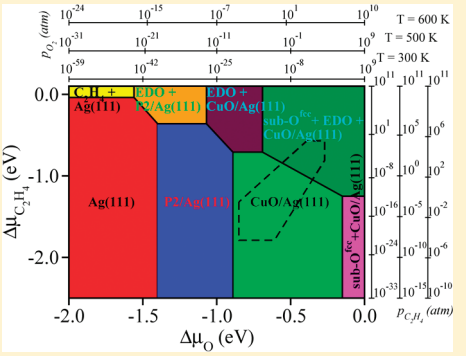

INTRODUCTION

Ethylene oxide, obtained through partial oxidation of ethylene, is an important compound for the chemical industry, because it is widely used as an intermediate for the production of chemicals such as ethylene glycol, which finds applications as an antifreeze and as a precursor to polymers. The oxidation of ethylene can lead either to the desired product (ethylene oxide, EO) or to the formation of acetaldehyde (Ac), which is readily converted to carbon dioxide, with the latter being the thermodynamically favored pathway. The optimal catalyst for this reaction should therefore selectively promote the formation of EO while avoiding total combustion. In the chemical industry the catalyst of choice for this process is silver.[1] While pure silver can reach a selectivity toward the production of EO of about 40−50%,[2] the inclusion of alkali and chlorine promoters can increase the selectivity of silver up to about 80%.[1,3,4]

Considerable efforts in the past few decades have been devoted to the understanding, at the atomic level, of the mechanism of metal-catalyzed ethylene epoxidation, because this could provide insights into the properties of the catalysts that more strongly affect their selectivity. Campbell[5] suggested the possibility of a common intermediate for both the pathway leading to EO and the one leading to total oxidation. Through temperature-programmed desorption (TPD) and high-resolution electron energy loss spectroscopy (HREELS), Linic and Barteau[6,7] have identified an oxametallacycle (OMC) intermediate on silver catalysts, where ethylene is bonded with one carbon atom to a surface metal atom and with the other carbon atom to oxygen, and proposed that an OMC is the common intermediate for both reaction paths. Several other intermediates have also been identified: Greely and Marvikakis,[8] through density functional theory (DFT) calculations, found that ethylenedioxy (EDO) could be present at the surface of silver catalyst under conditions of temperature and pressure compatible with the ones used experimentally.

Recently Linic and Barteau, through a combined theoretical and experimental work have shown that alloying silver with other metals, and in particular with copper, can lead to a substantial increase of the selectivity toward the formation of ethylene oxide.[9,10] However, while many studies have been devoted to the understanding of the mechanism of ethylene epoxidation process on monometallic catalysts,[5,11−16] the mechanism of the reaction on the bimetallic catalysts still remains unclear. Barteau and co-workers suggested that the mechanism found for monometallic systems holds also in the case of the Ag-based alloys they investigated.[9] They considered a catalyst model in which a surface alloy forms on top of Ag(111), obtained by replacing one out of four silver atoms with another metal atom. While this assumption could be reasonable in ultra-high-vacuum conditions, recent theoretical and experimental works involving some of us[17−19] have shown that such a structure is not predicted to be stable in an oxygen−ethylene environment at temperatures and pressures relevant for industrial applications. Copper, on the other hand, segregates to the surface and forms stable, thin oxide-like films. These studies show that temperature and pressure significantly

Received: January 17, 2011
Revised: April 15, 2011
Published: May 03, 2011

dx.doi.org/10.1021/jp200489e | J. Phys. Chem. C 2011, 115, 10073–10079

impact the structural properties of catalysts, and their effects on the reaction mechanism should not be excluded.

In these works, however, the effect of the ethylene atmosphere was accounted for only implicitly, by investigating the conditions of temperature and pressure under which the thin oxide would decompose into the pure metals, and ethylene would be converted to EO or Ac.[19] Here, we go beyond this approach, by explicitly accounting for the presence of ethylene on the surface of the catalysts. We consider several possible intermediate structures and study the phase diagram of the system in presence of both an oxygen and an ethylene atmosphere as a function of pressure and temperature. We also discuss the possible role of these intermediates on the catalytic mechanism on the basis of our previous results on this topic,[20] as well as the correlation between their formation and the geometry of catalyst particles.

METHODOLOGY

Our calculations are based on density functional theory (DFT) using the generalized gradient approximation (GGA) of Perdew–Burke–Ernzerhof (PBE)[21] for the exchange and correlation functional. We employ ultrasoft pseudopotentials[22,23] for the electron–ion interactions, including scalar relativistic effects. The Kohn–Sham wave functions are expanded in plane waves basis sets up to a kinetic energy cutoff of 30 Ry (300 Ry for the charge-density cutoff). Brillouin-zone integrations have been performed with the special-point technique,[24] smearing the Fermi surface through the Marzari–Vanderbilt cold-smearing technique,[25] using a smearing parameter of 0.03 Ry (0.41 eV). We model the catalysts, employing a periodically repeated slab geometry for the (111), (100), and (110) surface orientations, using a (2×2) surface supercell, with adsorbates on one side of the slab only. The Brillouin-zone integrations are performed with a $6 \times 6 \times 1$ Monkhorst–Pack[24] grid for the (111) and (100) surfaces, and with a $6 \times 4 \times 1$ grid for the (110) surface. The slabs are five layers thick (four Ag layers and one layer for the Cu/O adsorbates), and the bottom two layers of the slab are kept fixed in their bulk positions. A 12 Å vacuum layer is used, which is found to be sufficient to ensure negligible coupling between periodic replicas of the slab.

For the calculation of the reaction pathways and the transition state along the minimum energy path (MEP), we adopt the climbing-image nudged-elastic band (CI-NEB) method.[26] Relaxation during NEB minimization is performed for all atoms, except the bottom two layers that were kept fixed, until the forces are less than 0.01 eV/Å. All the calculations are performed using the PWscf code integrated in the Quantum-ESPRESSO distribution.[27]

To take into account the effects of temperature (T) and pressure (p), we use the constrained ab initio atomistic thermodynamics approach,[28−30] in which the system under investigation is considered to be in contact with the oxygen and ethylene reservoirs at fixed chemical potentials (i.e., at fixed temperature and partial pressure), while the two reservoirs do not interact with each other.

We define the free energy of adsorption as:

$$G^{ads}(\mu_O,\mu_{C_2H_4}) = G^{tot}_{slab} - G^{Ag}_{slab} - \Delta N_{Ag}\mu_{Ag} - N_{Cu}\mu_{Cu} - N_O\mu_O - N_{C_2H_4}\mu_{C_2H_4} \quad (1)$$

where G^{tot}_{slab} and G^{Ag}_{slab} are the Gibbs free energies of the total system (comprising ethylene and/or oxygen adsorbed on the Ag–Cu alloy surfaces) and the clean Ag surface, respectively. ΔN_{Ag} is the number of Ag atoms in addition to the ones contained in the slab, N_{Cu}, N_O, and $N_{C_2H_4}$ are number of Cu atoms, O atoms, and ethylene molecules, μ_{Ag}, μ_{Cu}, μ_O, and $\mu_{C_2H_4}$ are the chemical potentials of Ag, Cu, O, and ethylene, respectively. With this definition, lower values of adsorption free energies correspond to more stable structures.

The surface free energy of adsorption, $\gamma(\mu_O,\mu_{C_2H_4})$ is obtained by dividing G^{ads} by the area of the simulation cell. Vibrational and configurational entropy contributions can be assumed to be sufficiently small so as not to play an important role on the Ag–Cu oxidized surfaces,[17,29,30] which allows us to identify the free energies of the adsorption systems with their total energies. The chemical potentials of Ag and Cu are fixed at their bulk values. In the following, we will measure the chemical potential of oxygen and ethylene with respect to the molecular energies ($\Delta\mu_O = \mu_O - {}^1/_2E^{total}_{O_2}$) and ($\Delta\mu_{C_2H_4} = \mu_{C_2H_4} - E^{total}_{C_2H_4}$). The oxygen and ethylene chemical potentials depend on temperature and pressure according to:

$$\mu_O(T,p) = \frac{1}{2}[E^{total}_{O_2} + \Delta\mu_{O_2}(T,p^o) + kT\ ln(p/p^o)] \quad (2)$$

$$\mu_{C_2H_4}(T,p) = E^{total}_{C_2H_4} + \Delta\mu_{C_2H_4}(T,p^o) + kT\ ln(p/p^o) \quad (3)$$

Here, p^o is the standard pressure and $\Delta\mu(T,p^o)$ is the increment with respect to 0 K value of chemical potentials at the standard pressure, which can be obtained from thermochemical tables.[31]

RESULTS AND DISCUSSION

Adsorption of Ethylene on Ag–Cu Alloy Surfaces in a Reactive Environment

Ethylene Physisorption on Oxygen Precovered Ag–Cu Alloy Surfaces. The adsorption of the reactants on the catalyst surface is the first step of the mechanism of ethylene epoxidation that has been proposed on monometallic as well as on alloy catalysts.[11,16] Several theoretical studies, therefore, have examined adsorption of ethylene on both the clean and oxygen precovered Ag and Cu surfaces. For example, A. Kokalj et al.[32] found that ethylene adsorbs weakly (∼−0.1 eV) on the clean Ag surfaces. It has been also shown that the adsorption of ethylene is strongly promoted by the presence of subsurface oxygen[32] and Ag adatoms[33] as well as by positively charged Ag sites in Ag-oxide-covered Ag(111).[34] Analogously, the studies of ethylene adsorption on clean Cu surfaces show a similarly small binding energy in the $\theta_O = 1/16$ to 1/4 ML coverage range.

In the case of the Ag–Cu alloy in an oxygen environment, several surface structures with similar energetics have been predicted to form on the low-index surfaces of this material. Here we will focus on the two most stable structures with a (2×2) periodicity of the (111) facet labeled "P2" and "CuO", and on the "CuO" structures on the (100) and (110) facets.[17,18] In Figure 1a–d, we show the relaxed adsorption geometries of ethylene on these four surface structures.

Note that bulk CuO is poorly described with DFT-PBE: CuO is a strongly correlated antiferromagnetic semiconductor, with a monoclinic structure,[35] while DFT-PBE predicts CuO to be a metal with an almost orthorhombic structure.[17] We will, however, limit ourselves to one-layer thick CuO layers adsorbed on a metal, where we expect these shortcomings not to be as relevant as in the bulk phase.

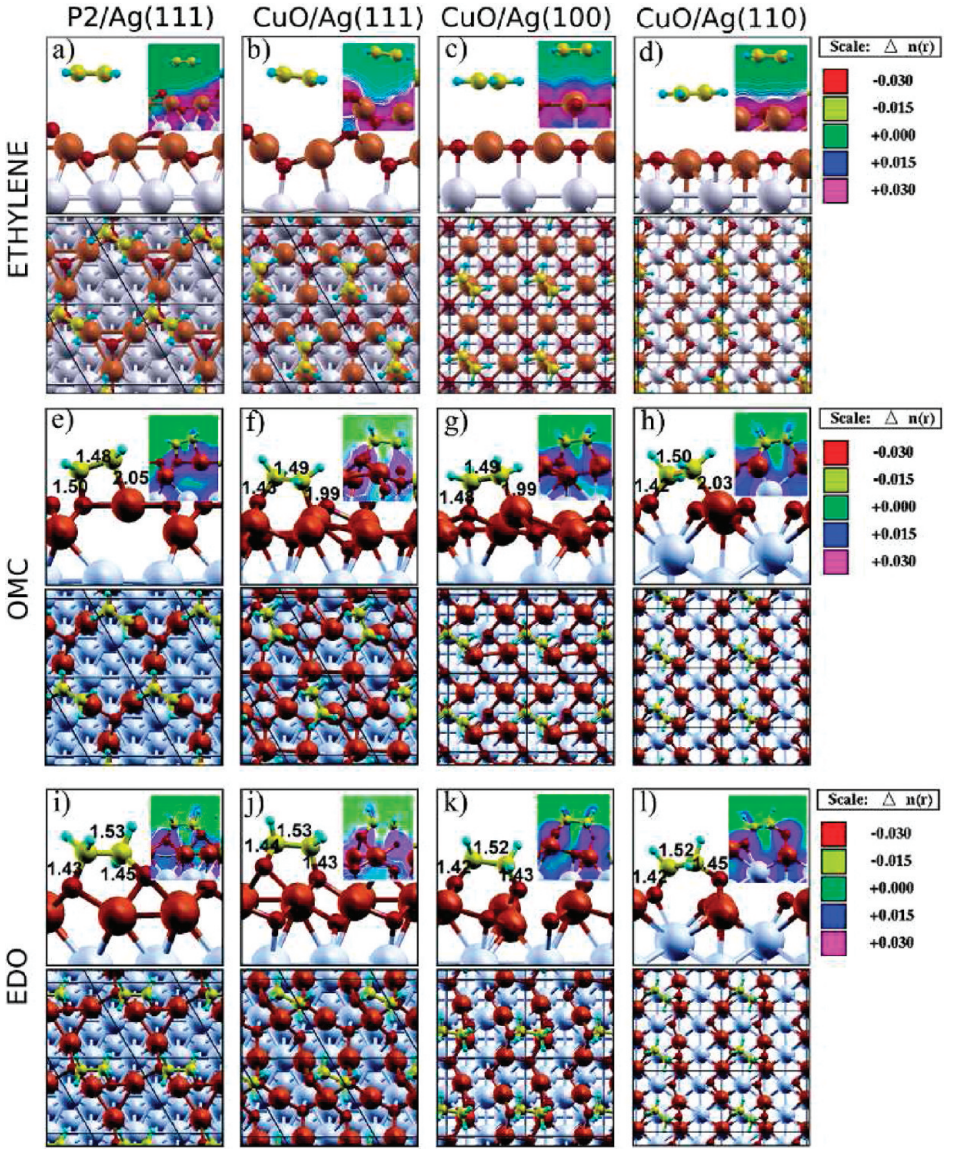

Figure 1. Top and side view of physisorbed ethylene (a−d) and chemisorbed ethylene for OMC configuration (e−h) and for EDO configuration (i−l) on the low energy structures considered in this work: P2 on the (111) surface and one layer of CuO on the (111), (100), and (110) surfaces. The small red atoms represent oxygen, the large brown ones represent copper, the large light gray ones represent silver, the small yellow ones represent carbon, and the small green ones represent H. The insets show the charge density difference for considered structures. Contours are drawn in linear scale from −0.03 to 0.03 e/Å^3 with the increment of 0.015 e/Å^3. The charge flows from the red to blue region.

The ethylene adsorption energy (defined as the zero temperature free energy of adsorption) on different surfaces is shown in Table 1. This quantity is almost unchanged on different orientations of Ag−Cu catalyst surfaces and comparable with that obtained in pure Ag and Cu. Consistently, we find that the geometry of adsorbed ethylene is unchanged with respect to the gas phase. The C−C length, for example, is in all cases 1.33 Å.

In Figure 1a−d, we also show the contour plot of the induced charge density, defined as $\Delta n(r) = n_{tot} - [n_{C_2H_4} + n_{surface}]$, i.e., the difference between the charge density of the adsorption system and the sum of the isolated ethylene and catalyst surface. This shows that there is no net charge transfer between ethylene and the surface and also indicates the lack of formation of any covalent interaction between ethylene and the surface, in agreement with the small adsorption energies predicted by our calculations.

Table 1. Adsorption Energy (in eV) of the Most Stable Physisorbed and Chemisorbed Ethylene Configurations on Ag−Cu Alloy Surfaces[a]

surface	C_2H_4	OMC	EDO	E_O^f
P2/Ag(111)	−0.07	0.86	−0.36	−0.97
CuO/Ag(111)	−0.10	0.33	−0.71	−1.06
CuO/Ag(100)	−0.08	0.53	−0.63	−1.09
CuO/Ag(110)	−0.04	−0.12	−1.01	−1.28

[a] The last column shows the formation energy per oxygen atom (in eV) of the thin oxide-like surface layers.

Here we point out that GGA functionals, however, do not provide a correct description of dispersion (i.e., van der Waals) interactions, which are the essential component of physisorption.

dx.doi.org/10.1021/jp200489e |J. Phys. Chem. C 2011, 115, 10073–10079

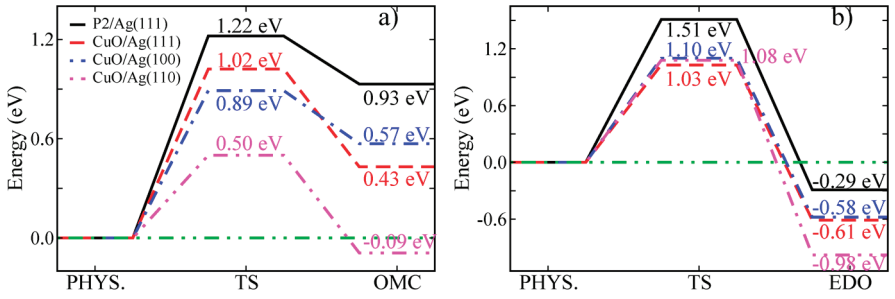

Figure 2. Reaction profiles for the formation of OMC (a) and EDO (b) on the most stable Ag−Cu alloy surfaces. The zero level is the energy of physisorbed ethylene on P2 and CuO structures at different surface orientations.

The computed adsorption energies are therefore likely underestimated (in absolute value).

Formation of Oxametallacycle. Because OMC has been found to be a common intermediate for both the selective and unselective paths on pure Ag(111),[11] we now investigate the stability of this configuration on the thin oxide-like layers that we predicted to be present in an oxidizing atmosphere. In Figure 1e−h, we display, for each of the four thin oxide-like layers considered in this work, the most stable OMC structure. The ethylene fragment in OMC can be seen as a di-σ-bonded ethylene with the first carbon atom linked to copper and with the second one bound to oxygen. Ethylene undergoes a change from sp^2 to sp^3 hybridization during the formation of OMC, which is evident from a reduction of the trans H−C−C−H dihedral angle and an elongation of the C−C bond. The former reduces from 180° in gas-phase ethylene to values ranging from 137° to 168°, depending on the surface orientation. These values are higher than those on the low oxygen-covered surfaces of pure Cu (108°) or Ag (116−120°) catalysts.[13,15] The C−C distances on the OMC configurations (1.48−1.49 Å) are elongated relative to the gas phase (1.33 Å) and are slightly smaller than those found for OMC on pure Ag (1.50 Å) and Cu (1.518 Å).

In Table 1, we show the adsorption energy of OMC relative to ethylene in the gas phase. The formation of OMC is exothermic only on the CuO/Ag(110) surface, while on the other three surface structures considered here, the formation of this intermediate is not energetically favorable. We found that the OMC adsorption energy correlates with the formation energy per oxygen atom of the these oxide layers (last column in Table 1). This suggests that the stability of the oxygen atoms in the oxide layers is the key factor in determining the energetics of OMC formation.

In Figure 2a, we show the energy profile of the OMC formation reaction, starting from the physisorbed ethylene configuration. We find that the activation energy, E^*, for the formation of OMC on the CuO/Ag(110) is only 0.5 eV, whereas on (111) and (100) surfaces, E^* = 1.02 and 0.89 eV, respectively. For the P2 structure on the (111) surface, we find an even higher value, E^* = 1.22 eV. From Figure 2a, we can see that the lowest activation energy corresponds to the most exothermic reaction, while the highest corresponds to the most endothermic, in agreement with the Brønsted−Evans−Polanyi relation that predicts a linear relationship between activation energy and reaction enthalpy.[36,37] We note, though, that this relation does not hold for the CuO/Ag(111) and CuO/Ag(100) structures; however, these two systems have similar energetics.

Formation of Ethylenedioxy. Another candidate intermediate in the ethylene epoxidation reaction is ethylenedioxy (EDO), where each of the two carbons in ethylene is bound to a chemisorbed oxygen atom. This structure and its single carbon analogue, methylenedioxy, have been observed experimentally through temperature programmed desorption (TPD) during ethylene glycol decomposition on the surface of a silver catalyst and through Fourier transform infrared (FTIR) spectroscopy and chemical trapping on the surface of copper supported on zinc aluminate upon adsorption of formaldehyde.[38−40]

First-principles simulations have shown that on pure Ag surfaces, EDO is formed when the oxygen coverage is increased to 1/2 ML.[8] Because the thin oxide layers we are considering here have a high oxygen content, EDO represents a likely intermediate also for these systems. In Table 1, we show the adsorption energy of EDO relative to gas-phase ethylene. Clearly this intermediate is considerably more stable than both physisorbed ethylene and OMC. We note, however, that the adsorption energies reported in Table 1 are zero-temperature values, while the effects of temperature and pressure will be analyzed in detail in the following.

In Figure 1i−l, we show the relaxed adsorption geometries for EDO. The C−C distances in the EDO on four surface structures are elongated compared to gas-phase ethylene and also compared to OMC. The trans H−C−C−H dihedral angles are strongly reduced with respect to the planar structure of ethylene. The dihedral angles are of 62°, 75°, 62°, and 48° for EDO on P2, CuO on (111), and CuO on (100) and (110), respectively. The induced charge density displayed in the insets of Figure 1i−l shows a large perturbation around the oxygen atoms, indicating the formation of strong C−O−metal bonds.

In Figure 2b, we show the reaction profile for the formation of EDO starting from physisorbed ethylene. The activation energies exceed, on all surface structures, 1.0 eV, suggesting that the formation of this stable intermediate might be kinetically hindered. We anticipate here that the activation energy to form either EO or AC starting from EDO is considerably higher than starting from other intermediates, indicating that the formation of EDO would poison the catalyst surface. As we will see in following section, EDO is predicted to be found at the surface of the alloy catalysts only at high ethylene partial pressure. This could be a possible explanation for the experimental observation that the activity of the catalyst is reduced as the ethylene partial pressure is increased.[10]

Thermodynamic Diagrams of Ag−Cu Alloy in Reactive Environment. Having established the relevant low energy structures formed by oxygen and ethylene on Ag−Cu alloy surfaces, we now turn to the surface phase diagrams of the (111), (100), and (110) surfaces. The key quantity is the surface free energy calculated as a function of chemical potentials of O and C_2H_4. The most stable structures are identified as the ones that minimize the surface free energy for a particular value of $\Delta\mu_O$ and $\Delta\mu_{C_2H_4}$.

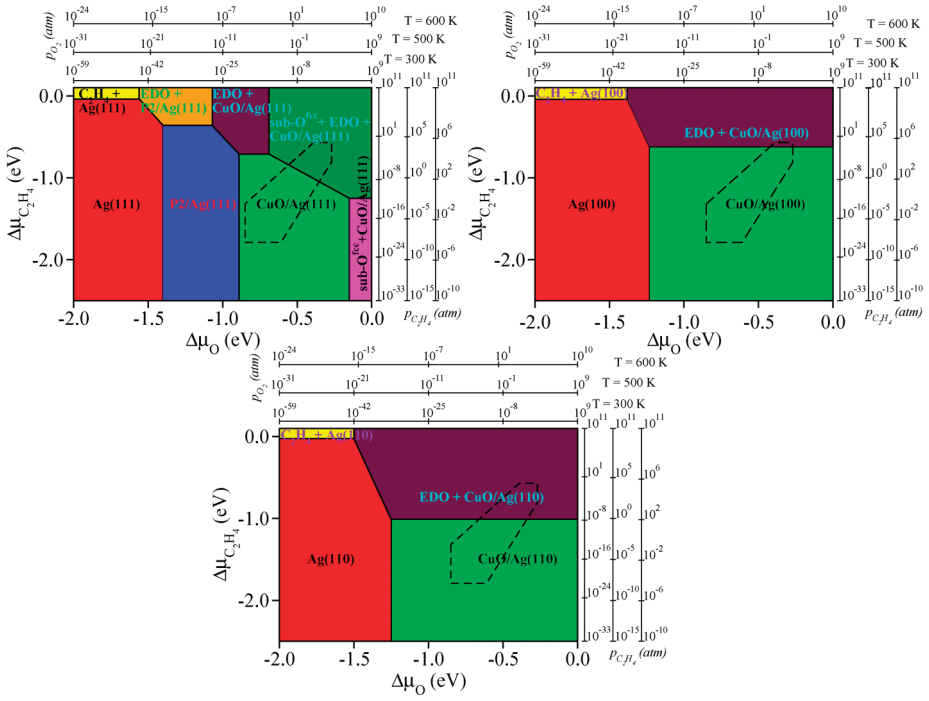

Figure 3. Surface phase diagrams of stable structures on Al−Cu alloy surfaces in equilibrium with oxygen and ethylene environments, as a function of $\Delta\mu_O$ and $\Delta\mu_{C_2H_4}$ in the gas phase. The additional axes show the corresponding pressure scales at T = 300, 500, and 600 K.

In ref 19, Piccinin et al. considered the stability of the thin oxide-like layers in the presence of the reducing agent (ethylene), while neglecting the possibility of physisorbed or chemisorbed ethylene (which, as we show below, is correct for values of temperature and oxygen/ethylene pressure used experimentally). They showed that, in agreement with experimental findings, the oxidation of ethylene to either EO or AC does not reduce the oxide layers to metallic copper. Here we extend this study by explicitly considering physisorbed and chemisorbed ethylene structures on these layers and studying their relative stability as a function of temperature and partial pressure of both oxygen and ethylene.

In this section, we consider the surface free energy of adsorption of the ethylene structures (OMC and EDO) on clean Ag, the thin oxide-like CuO/Ag and P2/Ag, and their subsurface oxygen structures, on the (111), (100), and (110) surfaces. In total we have studied 47 different surface structures. Projecting the lowest surface energies on the $(\Delta\mu_O,\Delta\mu_{C_2H_4})$ plane, we obtain the surface phase diagrams of the thermodynamically most stable configurations (Figure 3). In these graphs we also report, for three values of temperature (300, 500, and 600 K), the values of partial pressure for oxygen and ethylene corresponding to the chemical potentials shown on the axis.

Analyzing these phase diagrams, we note that, as expected, at low values of ethylene chemical potential (i.e., low ethylene partial pressure or high temperature), the stable structures do not contain ethylene. In these regimes we therefore recover the phase diagram of the O/Ag/Cu system already investigated in previous publications.[17,18] As the value of the ethylene chemical potential is raised, the first ethylene-containing structures that appear in the phase diagram contain EDO, on all three facets. This reflects the stability of EDO intermediates already highlighted in Table 1.

Physisorbed ethylene is found to be stable only at high ethylene and low oxygen chemical potentials, and only on pure Ag surfaces, on all three facets. This can be understood because at low values of $\Delta\mu_O$ the formation of oxygen-containing EDO and oxide-like structures is disfavored. Of particular interest are the thermodynamic conditions close to the experimental values of temperature and partial pressures used in real catalysis. These roughly correspond to T = 500−600 K and pressures in the range of a few atmospheres.[41] In Figure 3, we show with a dashed polygon the area corresponding to T = 300−600 K and pressures in the 10^{-4}−10^{0} atm range. The conditions that more closely resemble the surface science experimental setups are found in the lower-left corner of the polygon, while industrial conditions correspond to the central region of the polygon. Around this point, on all three facets, we find the CuO/Ag structure, while at the lower temperature and higher pressure end of the polygon, we find EDO chemisorbed on the thin oxide-like CuO/Ag of (100) and (110) surfaces, and on the subsurface oxygen structure of the thin oxide-like CuO/Ag of the (111) surface. We recall here that EDO has been predicted to be present also in the phase diagram of pure Ag(111) under conditions of temperature and partial pressures compatible with those used experimentally.[8] We have shown in an earlier work[20] that once EDO is formed, the kinetic barrier toward the formation of the final products is very high (1.84 eV in the case of the P2/Ag(111)). This intermediate would therefore poison the catalyst surface. Fixing the partial pressures of both oxygen and ethylene to 1 atm, our calculations predict that this intermediate would be present on the CuO/Ag(110) surface below 480 K, on the CuO/Ag(100) surface below 323 K, on the subsurface oxygen structure of CuO/Ag(111) surface below 475 K, and on the P2/Ag(111) surface below 208 K.

As already mentioned previously, OMC has been experimentally found to be a common intermediate for the conversion of ethylene to both EO and AC.[2,7] It is therefore important to stress that our calculations predict that this intermediate is not the most stable structure under any value of chemical potential of ethylene and oxygen. It has been argued that the presence of OMC

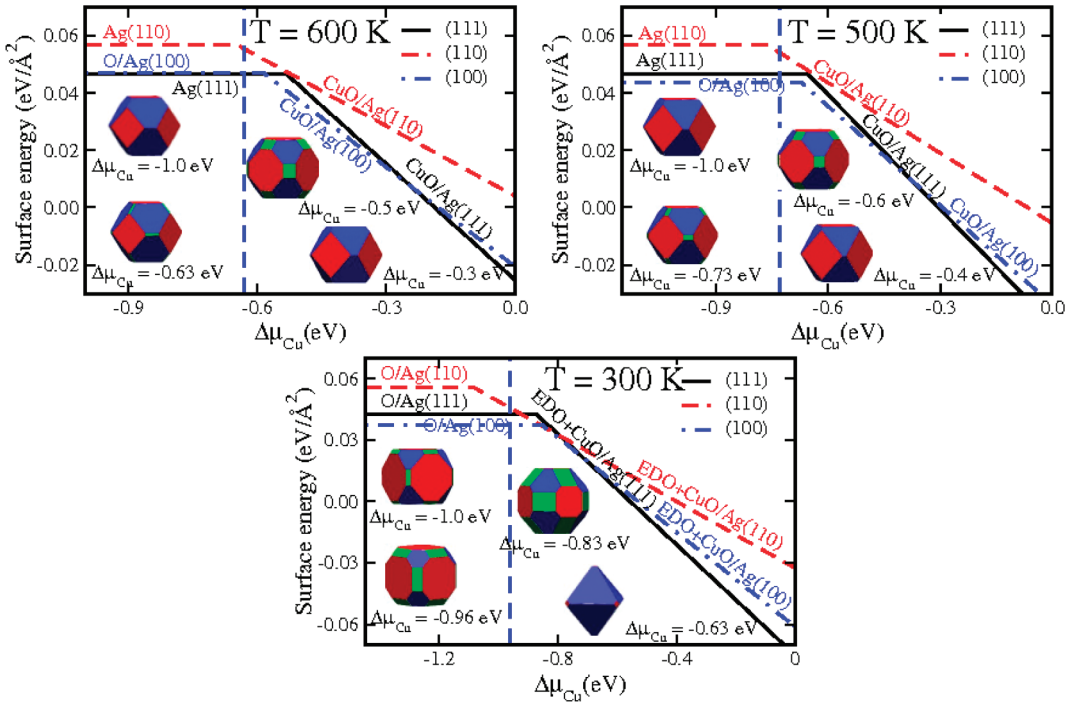

Figure 4. Surface free energies of the most stable surface structures on each of three surface orientations as a function of the Cu chemical potential. At selected Cu chemical potentials, also a model of a catalyst particle obtained through the Wulff construction is presented. $\Delta\mu_O$ and $\Delta\mu_{C_2H_4}$ are set to the values corresponding to T = 300, T = 500 and T = 600 K, and $p_{O_2} = p_{C_2H_4}$ = 1 atm.

intermediate on pure Ag surfaces might be stabilized at high oxygen chemical potential in the presence of subsurface oxygen.[8] To test this possibility, we considered the presence of subsurface oxygen and verified that, even in this case, OMC is not present in the phase diagram.

Geometry of Ag−Cu Alloy Catalysis Particles as Known Cu Surface Content. Recently, experiments have showed that the catalytic selectivity in ethylene epoxidation of ethylene to form ethylene oxide on alumina-supported silver catalysts depends on both reaction conditions and geometric structure of catalytically active Ag particles.[42] Indeed, the selectivity to EO on Ag nanowire catalysts is much higher than that on conventional Ag particles with similar external conditions. The enhanced EO selectivity of the nanowire catalysts is attributed to the higher concentration of the Ag(100) surface facets on the nanowire in comparison to Ag particles.[42−45] Density functional theory calculations also showed that the Ag(100) surface facet is inherently more selective toward EO than toward the Ag(111).[2,46] It is therefore important to study how the shape of the particles depends on the ambient conditions and on the copper content. To this end, we use the Wulff construction to predict the shape of the particle that minimizes its total surface free energy. We fix the value of the chemical potentials of both ethylene and oxygen corresponding to partial pressures $p_{O_2} = p_{C_2H_4}$ = 1 atm, and to three values of temperature, T = 300, 500, and 600 K. The chemical potential of Cu measured relative to its bulk value, $\Delta\mu_{Cu}$, will be used as a parameter that controls the amount of Cu in the particle. Low values of $\Delta\mu_{Cu}$ correspond to Cu-lean conditions, while high values correspond to Cu-rich conditions. In Figure 4, the vertical dashed lines represent the Cu chemical potential above which Cu oxidizes to bulk copper oxide, which, as one can show, corresponds to the computed heat of formation of bulk copper oxide at the fixed value of oxygen chemical potential.

In Figure 4, we show, for three values of temperature, the surface free energy of the most stable structure found on each of the three facets as a function of $\Delta\mu_{Cu}$. For selected values of $\Delta\mu_{Cu}$, we plot the shape of the particle predicted through the Wulff construction. Because experimentally the Cu surface content is found to be in the 0.1−0.75 ML range,[9,10] the values of $\Delta\mu_{Cu}$ compatible with these findings are those when some of the facets start being covered by thin copper oxide-like layers. The values of $\Delta\mu_{Cu}$ for which this happens is not far from the bulk copper oxide formation boundary. Taking into consideration our computational error-bars and kinetic effects, we can therefore expect some competition between bulk copper oxide and CuO/Ag surface formation, reflecting the fact that the formation energy of the thin layers is similar to their bulk counterpart.

Examining the surface free energy plots in Figure 4 at T = 600 K, we can see that, as $\Delta\mu_{Cu}$ is increased, the first facet to be covered by the thin layers is the (110), while as soon as all the facets are oxidized, the lowest energy surface is the (100). This is particularly relevant because in pure Ag the lowest energy surface is the (111), while the most selective is the (100). Our calculations show that the inclusion of copper has the effect of lowering the surface free energy of the (100) facet relative to the other low-index facets, and we therefore predict that Cu-containing catalyst particles should expose a larger fraction of (100) area compared to pure Ag.

This effect is, on the other hand, reversed at lower temperature. Looking at the T = 300 K case in Figure 4, we can see that as soon as all facets are covered by thin oxide layers, the (100) facet is not dominant. In this case all facets are covered by EDO chemisorbed on CuO/Ag and, as reported in Table 1, EDO binds more strongly to the (110) and (111) surface compared to the (100) one, therefore lowering their surface free energy relative to the (100).

CONCLUSIONS

By means of ab initio atomistic thermodynamics, we have investigated the structural properties and the energetics of candidate intermediates in the ethylene epoxidation reaction catalyzed by Ag−Cu alloys. By considering the system to be in constrained equilibrium with oxygen and ethylene reservoirs, we were able to identify the most stable surface structures on the low-index surfaces as a function of temperature and partial pressures. We found that around values of temperature and partial pressures relevant for industrial applications, the catalyst is formed, on all three facets examined, by a thin CuO oxide-like layer on top of pure Ag. At lower temperature or higher partial pressures, these surface structures are covered by the EDO, where ethylene binds to the surface via two oxygen atoms. Moreover we predict that, under these conditions, on the (111) surface, subsurface oxygen will be present at the interface between the CuO layer and the silver slab. Our calculations also indicate that around 600 K and for Cu contents below one monolayer, the (100) facet becomes dominant. At lower temperatures, where the facets are covered by EDO, the (111) facet is the dominant one.

We found that OMC, a proposed common intermediate for both the selective and unselective reaction paths in pure metal catalysts, is not present on the phase diagrams of any facets under any condition of temperature and partial pressures. This is due to the considerably higher stability of the EDO intermediate compared to OMC. This could have important implications for the mechanism of reaction, because the conversion of EDO to either EO or Ac is a highly activated process.[20]

AUTHOR INFORMATION

Corresponding Author
*E-mail: nnlinh@sissa.it.

ACKNOWLEDGMENT

Calculations were performed at SISSA and at CINECA computing center in Bologna.

REFERENCES

(1) van Santen, R. A. *Handbook of Heterogeneous Catalysis*; Wesley: Weinheim, Germany, 1997; Vol. 5; Chapter 4.6.1, p 2244.
(2) Linic, S.; Barteau, M. A. *J. Am. Chem. Soc.* **2003**, *125*, 4034–4035.
(3) Serafin, J. G.; Liu, A. C.; Seyedmonir, S. R. *J. Mol. Catal. A: Chem.* **1998**, *131*, 157–168.
(4) Lambert, R. M.; Williams, F. J.; Cropley, R. L.; Palermo, A. *J. Mol. Catal. A: Chem.* **2005**, *228*, 27–33.
(5) Campbell, C. T. *J. Catal.* **1985**, *94*, 436–444.
(6) Linic, S.; Barteau, M. A. *J. Am. Chem. Soc.* **2002**, *124*, 310–317.
(7) Luskaski, A. C.; Barteau, M. A. *Catal. Lett.* **2009**, *128*, 9–17.
(8) Greeley, J.; Mavrikakis, M. *J. Phys. Chem. C* **2007**, *111*, 7992–7999.
(9) Linic, S.; Jankowiak, J. T.; Barteau, M. A. *J. Catal.* **2004**, *224*, 489–493.
(10) Jankowiak, J. T.; Barteau, M. A. *J. Catal.* **2005**, *236*, 366–378.
(11) Linic, S.; Barteau, M. A. *J. Am. Chem. Soc.* **2003**, *125*, 4034–4035.
(12) Stegelmann, C.; Schidt, N. C.; Campbell, C. T.; Stoltze, P. *J. Catal.* **2004**, *221*, 630–649.
(13) Torres, D.; Lopez, N.; Illas, F. *J. Catal.* **2006**, *243*, 404–409.
(14) Torres, D.; Illas, F. *J. Phys. Chem. B* **2006**, *110*, 13310–13313.
(15) Kokalj, A.; Gava, P.; de Gironcoli, S.; Baroni, S. *J. Phys. Chem. C* **2008**, *112*, 1019–1027.
(16) Kokalj, A.; Gava, P.; de Gironcoli, S.; Baroni, S. *J. Catal.* **2008**, *254*, 304–309.
(17) Piccinin, S.; Stampfl, C.; Scheffler, M. *Phys. Rev. B* **2008**, *77*, 075426–075435.
(18) Piccinin, S.; Stampfl, C.; Scheffler, M. *Surf. Sci.* **2009**, *603*, 1467–1475.
(19) Piccinin, S.; Zafeiratos, S.; Stampfl, C.; Hansen, T. W.; Havecker, M.; Teschner, D.; Bukhtiyarov, V. I.; Girgsdies, F.; Knop-Gericke, A.; Schlögl, R.; Scheffler, M. *Phys. Rev. Lett.* **2010**, *104*, 035503–035507.
(20) Piccinin, S.; Nguyen, N. L.; Stampfl, C.; Scheffler, M. *J. Mater. Chem.* **2010**, *20*, 10521–10527.
(21) Perdew, J. P.; Burke, K.; Ernzerhof, M. *Phys. Rev. Lett.* **1996**, *77*, 3865–3868.
(22) Vanderbilt, D. *Phys. Rev. B* **1990**, *41*, 7892–7895.
(23) The ultrasoft pseudopotentials for Ag, Cu, O, C, and H were taken from the QUANTUM-ESPRESSO pseudopotential download page: http://www.quantum-espresso.org/pseudo.php (files: Ag.pbe-d-rrkjus.UPF, Cu.pbe-d-rrkjus.UPF,O.pbe-rrkjus.UPF, C.pbe-rrkjus.UPF, and H.pbe-rrkjus.UPF).
(24) Monkhorst, H. J.; Pack, J. D. *Phys. Rev. B* **1976**, *13*, 5188–5192.
(25) Marzari, N.; Vanderbilt, D.; Vita, A. D.; Payne, M. C. *Phys. Rev. Lett.* **1999**, *82*, 3296–3299.
(26) Henkelman, G.; Uberuaga, B. P.; Johnson, H. *J. Chem. Phys.* **2000**, *113*, 9901–9904.
(27) Giannozzi, P.; Baroni, S.; Bonini, N.; Calandra, M.; Car, R.; Cavazzoni, C.; Ceresoli, D.; Chiarotti, G. L.; Cococcioni, M.; Dabo, I.; *J. Phys.: Condens. Matter* **2009**, *21*, 395502–395520.
(28) Stampfl, C. *Catal. Today* **2005**, *105*, 17–35.
(29) Reuter, K.; Scheffler, M. *Phys. Rev. B* **2001**, *65*, 035406–035417.
(30) Li, W. X.; Stampfl, C.; Scheffler, M. *Phys. Rev. B* **2003**, *67*, 045408–045424.
(31) Prophet, H.; Stull, D. R. *JANAF Thermochemical Tables*, 2nd ed.; US National Bureau of Standards: Washington, DC, 1971.
(32) Kokalj, A.; Dal Corso, A.; de Gironcoli, S.; Baroni, S. *Surf. Sci.* **2003**, *532*, 191–197.
(33) Kokalj, A.; Dal Corso, A.; de Gironcoli, S.; Baroni, S. *J. Phys. Chem. B* **2002**, *106*, 9839–9846.
(34) Bocquet, M. L.; Sautet, P.; Cerda, J.; Carlisle, C. I.; Webb, M.; King, D. A. *J. Am. Chem. Soc.* **2003**, *125*, 3119–3125.
(35) Kim, J. Y.; Rodriguez, J. A.; Hanson, J. C.; Frenkel, A. I.; Lee, P. L. *J. Am. Chem. Soc.* **2003**, *125*, 10684–10692.
(36) Brønsted, N. *Chem. Rev.* **1928**, *5*, 231–338.
(37) Evans, M. G.; Polanyi, N. P. *Trans. Faraday Soc.* **1938**, *34*, 11–24.
(38) Capote, A. J.; Madix, R. J. *J. Am. Chem. Soc.* **1989**, *111*, 3570–3577.
(39) Bulushev, D. A.; Paukshtis, E. A.; Nogin, Y. N.; Bal'zhinimaev, B. S. *Appl. Catal. A: Chem.* **1995**, *123*, 301–322.
(40) Idriss, H.; Hindermann, J. P.; Kieffer, R.; Kiennemann, A.; Vallet, A.; Chauvin, C.; Lavalley, J. C.; Chaumette, P. *J. Mol. Catal.* **1987**, *42*, 205–213.
(41) Kollar, J.; Process for the industrial production of ethylene oxide and aromatic acid, United States 4046782, 1977, URL http://www.freepatentsonline.com/4046782.html.
(42) Christopher, P.; Linic, S. *ChemCatChem* **2010**, *2*, 78–83.
(43) Sun, Y.; Xia, Y. *Science* **2002**, *298*, 2176–2179.
(44) Chen, J.; Herricks, T.; Xia, Y. *Angew. Chem., Int. Ed.* **2005**, *44*, 2589–2592.
(45) Sun, Y.; Mayers, B.; Herricks, T.; Xia, Y. *Nano Lett.* **2003**, *3*, 955–960.
(46) Christopher, P.; Linic, S. *J. Am. Chem. Soc.* **2008**, *130*, 11264–11265.